Ulysses Data System
Kiel Electron Telescope Description

Institut für Experimentelle und
Angewandte Physik der
Christian-Albrechts-Universität
zu Kiel

PI: Bernd Heber, (heber@physik.uni-kiel.de)
Former PI: Horst Kunow, (hkunow@physik.uni-kiel.de)
TM: Reinhold Müller-Mellin, (mueller-mellin@physik.uni-kiel.de)

Kiel,

March 2, 2009

Chapter 1

The Kiel Electron Telescope Sensor System

Figure 1.1 (A) shows the location of the different scientific instruments on Ulysses. The antenna is pointing towards the Earth and corresponds to the axis of rotation. The Kiel Electron Telescope (KET) is part of the Ulysses COsmic ray and Solar Particle INvestigation (COSPIN) experiment, which has been described in detail by Simpson et al. [1992]. The arrow show the location of the COSPIN instrument group onboard the spacecraft. The different sensor units of the COSPIN consortium are shown in figure 1.1 (B). The KET (3) is mounted below the Low Energy Telescope (1), the Anisotropy Telescope (1), the High Energy Telescope (2) and the High Flux Telescope (4). Figure 1.1 (C) displays the flight spare model sensor unit and the electronic box of the KET. For comparison a five German mark coin is shown to demonstrate the size of the instrument. Figure 1.1 (D) shows a schematic sketch of the KET sensor system. D1 and D2 are 0.5 mm thick semiconductor detectors, C1 is an aerogel Cerenkov-detector and A a plastic anticoincidence scintillator. C2 is a lead fluoride Cerenkov-detector, S1 and S2 are plastic scintillators.

Functionally, the detector system consists of two parts: an entrance telescope and a calorimeter, surrounded by a guard counter A.

The entrance telescope is composed of a silica-aerogel Cerenkov-detector C1 inserted between semiconductor detectors, D1 and D2. Together with the guard counter A, this combination defines the geometry, selects particles with velocity $\beta > 0.938$ and determines the particle charge.

The calorimeter consists of a 2.5 radiation length lead-fluoride (PbF2) crystal used as Cerenkov-detector (C2) and a scintillator S2. In C2

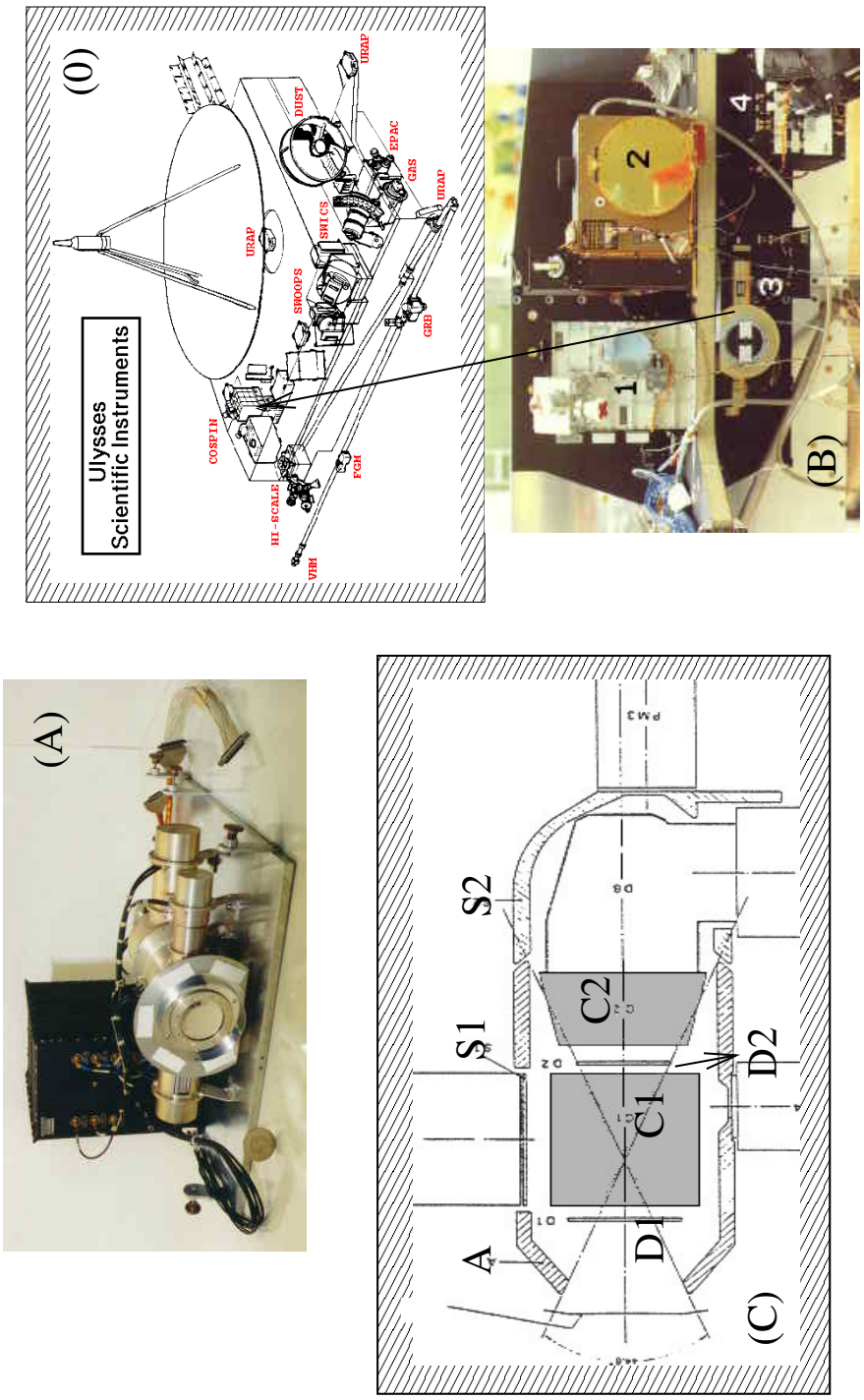

Figure 1.1: (A) Location of the scientific instruments onboard Ulysses, (B) mounting of the COSPIN sensor units, (C) flight spare model sensor unit of the Ulysses Kiel Electron Telescope (KET) with electronics box, and (D) cross section of the KET.

Name	Logic	primary particles	energy range (MeV/N)	Response[1]-factor (cm^2 sr MeV/N)	sectors
K1 (P1)	D11 $\overline{\text{D12 C10 D20 C20 S20 A0}}$	p	2.7-5.4	17.6	—
		p	23.1-34.1	71.5	
		He	2.3-2.7	2.6	
K21-K28 (P4)	D12 $\overline{\text{D13 C10 D20 C20 S20 A0}}$	p	5.4-23.1	115	8
		He	2.7-6.0	15	
		He	20.4-34.2	89.7	
K3 (P32)	D11 D20 $\overline{\text{D12 C10 C20 S20 A0}}$	p	34-125	70^d	—
K34 (P116)	D10 D20 S20 $\overline{\text{D12 C10 C20 A0}}$	p (F)	125-250	+	—
		p (B)	160-260	152^d	—
		He	126-190		
K12 (P190)	D10 D20 S20 C20 $\overline{\text{D11 C10 D21 C21 A0}}$	p	250-2200	3300	—
K10 (P4000)	D10 C10 D20 S20 C20 $\overline{\text{D11 C11 D21 C21 A0}}$	p	>2200	I	—
K2 (A4)	D13 $\overline{\text{C10 D20 C20 S20 A0}}$	He	5.4-23.1	115	—
K33 (A32)	D12 D21 $\overline{\text{D13 C10 C20 S20 A0}}$	He	34-125	70.0^d	—
K29 (A116)	D12 D21 S20 $\overline{\text{D13 C10 C20 A0}}$	He (F)	125-155	+	—
		He (B)	155-225	88	—
K31 (A190)	D11 D21 S20 C20 $\overline{\text{D12 C10 A0}}$	He	250-2100	3200	—
K30 (A4000)	D11 C10 D21 S20 C20 $\overline{\text{D12 C11 C21 A0}}$	He	>2100	I	—
K13-20 (E4)	D10 C10 D20 $\overline{\text{D11 C11 C20 S20 A0}}$	e	4-9	tbd	8
K11 (E12)	D10 C10 D20 C20 $\overline{\text{D11 C11 D21 S20 A0}}$	e	9-500	tbd	—
K32 (E300)	D10 C10 D20 C21 S20 $\overline{\text{D11 C11 D21 A0+A1}}$	e	>500	tbd	—

Table 1.1: KET coincidence channels. For each coincidence channel (Name) the logic is given. In addition to the detector denotations in the text a second digit is used here to indicate energy thresholds. Different particle species may trigger one or the other channel. For each of these primary particle types the energy range and the response factor is given. Response factors marked by ^{d} are only applicable to the PHA corrected daily averages and contain forward and backword penetrating particles for K34, K12, K29, and K31. If the energy range is different for backward and forward penetrating particles these ranges are given too. For the integral channel (protons and α-particles $>\sim$2 GeV/n) no response factor is given. Because of its strong energy dependence, no response factor is given for the electron channels (cf. text for details).

an electromagnetic shower can develop. The number of electrons leaving the PbF2-crystal are counted in S2.

The KET is designed to measure electron, proton and α-particle fluxes in several energy windows ranging from a few MeV/n up to and above a few GeV/n. The values listed in table 1.1 are based on a Monte Carlo simulation, as described below. The coincidence name and trigger condition are displayed in the first two columns. The particles and their corresponding energy range are listed in columns three and four. The response factor $R = C/I$, with C and I the counting rate and particle intensity, as well as the sectorization information of the coincidence channels are in columns five and six. For a statistical amount of measured particles the energy loss in the semiconductor detectors (D1 and D2) and the number of photons in the light detectors (C1,

C2, and S2) are transmitted. This information has been used to apply a pulse height analysis (PHA) for the channels K34, K12, K29, and K31. Factors marked by ^{d} are only applicable to this PHA corrected daily averages and contain forward and backword penetrating particles for K34, K12, K29, and K31. If the energy range is different for backward and forward penetrating particles, these ranges are given too. For the integral channel (protons and α-particles $>\sim$2 GeV/n) no response factor is given. In contrast to protons and α-particles, the response to electrons depends strongly on their energy within each coincidence channel. For that reason no response factor is given for the electron channels.

Chapter 2

Monte Carlo simulation of the KET

A treatment of the response functions of particle telescopes, and a number of exact formulae for multi-element telescopes have been given by Sullivan [1971]. However, the determination of the response function of rather complex telescopes like the KET instrument makes a Monte Carlo simulation mandatory. We assume that the differential coincidence counting rate of a particle telescope can be expressed as:

$$dC_{i,k} = dE\ R_i^k(E)\ J_k(E)(\text{counts/s}) \tag{2.1}$$

where $dC_{i,k}$ is the differential coincidence counting rate in channel i, $J_k(E)$ the flux of particle species k with kinetic energy E, and $R_i^k(E)$ the response function for particle species k in channel i, to be determined by the simulation. To get the counting rate C_i for the channel i we have to integrate over E and sum up for all particle species. In general, the response function may depend on many variables like the angular distribution of the incident particle flux, the location where a particle penetrates a detector etc. Here we assume that $R(E)$ is a function only of kinetic energy, valid for particle fluxes which are almost isotropic over the effective opening angle, and that the simulation properly averages over all other dependencies.

The Monte Carlo simulation was performed with the CERN Library Program GEANT 3 [Brun et al., 1987]. Particles were followed down to a low energy cutoff (electrons and gamma-rays 50 keV, protons 300 keV). Once reaching this cutoff, the particles were considered to be stopped and to have deposited all of their kinetic energy in the traversed material. The geometry of the detectors, mountings, foils, and the relevant structure material as well as the energy resolution of the readout electronics were accounted for in the simulation.

KET geometry: The model of the KET sensor unit in the simulation is shown in Figure 2.1. Shown are three possible tracks of 120 MeV protons. Two of these tracks are triggering the channel P32 and one of them is counted in P116.

Energy loss distribution: In addition to the count rates in all coincidence channels, the energy losses in D1 and D2 as well as the number of photons in C1, C2 and S2 are transmitted. Particle instruments are calibrated by using a particle beam provided by an accelerator [Sierks, 1988]. In space, particles of different species, incident directions and energies are observed nearly simultanously. Such an environment can not be simulated at an accelerator but can be simulated using an appropriate computer model. As an example figure 2.2 shows the simulated energy distribution of isotropic protons and α-particles in the semiconductor detectors D1 and D2 triggering the P32 and A32 coincidence channels. The D1-D2 PHA distribution (energy loss) has been calculated by using an uniform proton and α energy spectrum and an isotropic distribution. Solid lines in figures 2.2 show the mean energy losses. Marked on these lines are the expected energy losses for protons and α-particles with energies of 35, 40, 50, 70 and 120 MeV/n. The horizontal and vertical dotted lines display the electronics thresholds. In comparison, figure 2.3 shows a PHA distribution measured in space in January 1991. The entries below the dotted line could be identified as background. As is discussed in detail in Heber [1997], the proton and α-tracks in that matrix are well described by the GEANT Monte Carlo simulation.

2.1 Background contribution

Comparing figure 2.2 and 2.3 with each other, it is obvious that other particles contribute to the inflight measurements. In order to minimize the contribution of this background, masks in the D1-D2 pulse height distribution are defined. As an example the masks choosen for K3 (P32) and K33 (A32) as well as K34 (P116) and K29 (A116) are shown in figure 2.4 and 2.5, respectively.

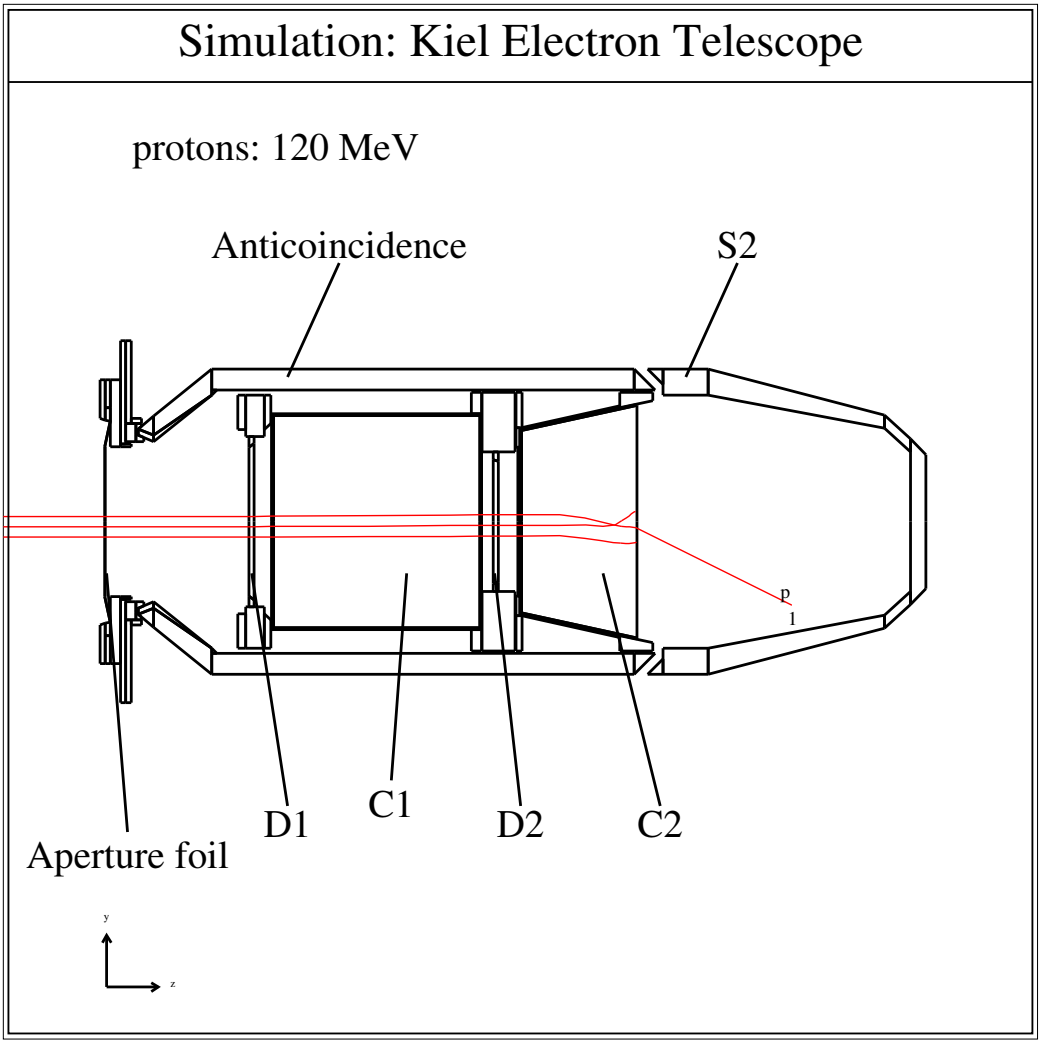

Figure 2.1: Model of the KET-detector stack in the GEANT simulation.

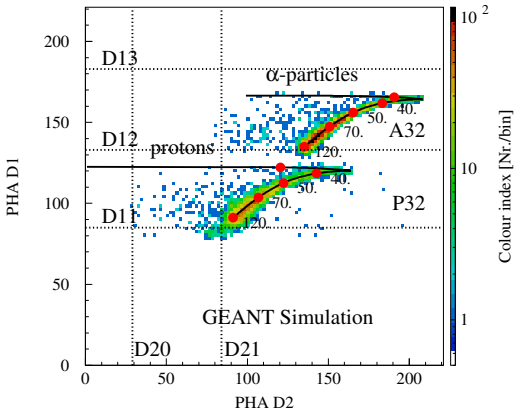

Figure 2.2: Simulated pulse height distribution in detector 1 over 2 in K3 (P32).

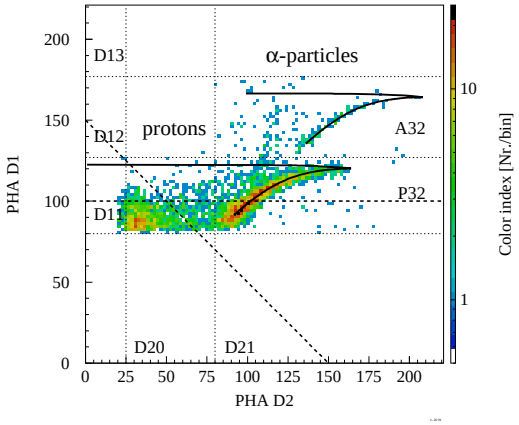

Figure 2.3: Measured pulse height distribution in detector 1 over 2 in K3 (P32).

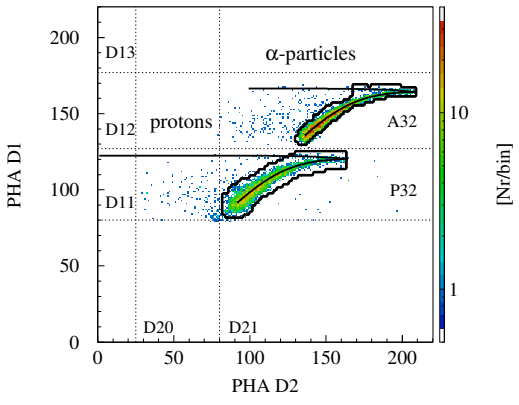

Figure 2.4: Correction masks for K3 (P32) and K33 (A32).

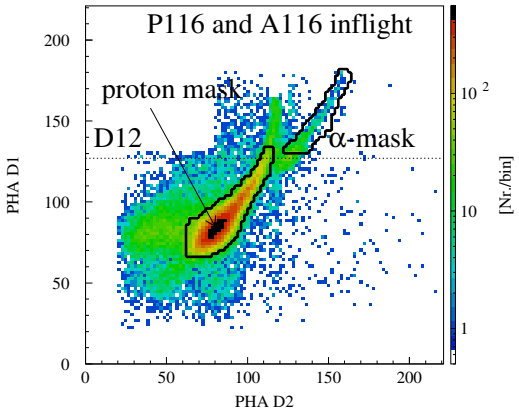

Figure 2.5: Correction masks for K34 (P116) and K29 (A116).

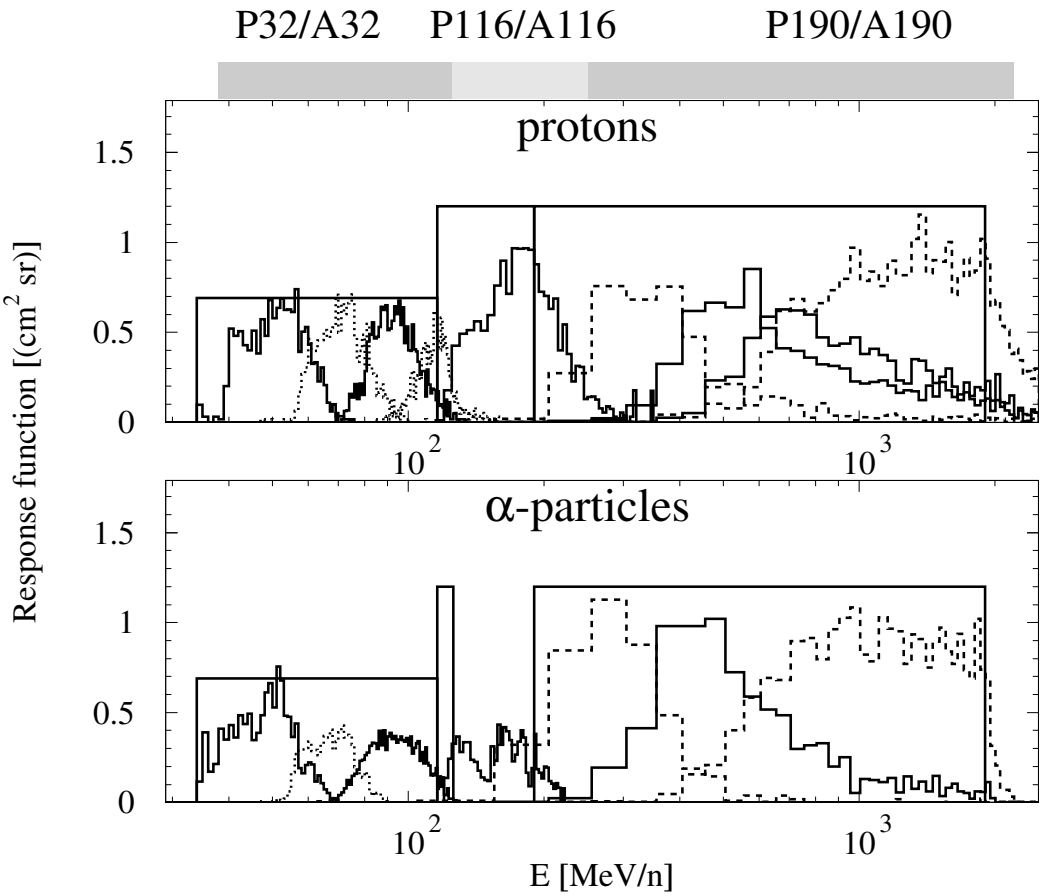

Figure 2.6: Response function of different KET coincidence channels, as defined in table 1.1.

2.2 Response factor

An important result of the analysis are the determination of the response of the instrument as a function of energy and particle species.

The response functions $R_i^{Sim}(E)$ for isotropic protons and α-particles are displayed in figure 2.6. The rectangular boxes indicate the response functions expected by using the Sullivan [1971] theory. For the low energy channels (K1, K21-K28, and K2) this theory is a good approximation. For the complex channels K3 (P32) to K10 (P4000) and K33 (A32) to K32 (E300) this approximation is not valid and one has to rely on the result of the Monte Carlo simulation. Since the shape of the

response function is not rectangular anymore, the response factor, the integral R_i over all energies of the response function, has to be used for each coincidence i. The intensity I follows from the measured count rates by dividing C_i by R_i.

Chapter 3

10 min averages readme

This readme was last modified March 2, 2009 and shall explain the file structure of the KET files provided for the Ulysses Data System (UDS). The previous sections "The Kiel Electron Telescope Sensor System" and "Monte Carlo simulation of the KET" explain the instrument. Only count rates are provided for the UDS. The geometrical factors provided in the previous section should be checked against the values on our homepage:

http://www.ieap.uni-kiel.de/et/ag-heber/cospin/

All UDS files have the name

UCOSKETAYYDOY.DAT

Herein YY is the year (eg. 90) and DOY the day of the year (eg. 365 of year 90 is 31.12.90).

3.1 Record format for the KET

The KET files are written on a VMS machine using Fortran 77 routines. The format used is:

```
      IMPLICIT REAL(K)
      CHARACTER*40 UDSKETFILE

          open(40,file=UDSKETFILE,
     1          form='formatted',
     2          RECL=125,
     3          iostat=ioS,
     4          status='NEW')
```

```
            WRITE(40,'(6I5)') IYEAR,IDOY,IHOUR,IMIN,ISEC,ICOV
            WRITE(40,'(10G11.3)')
     1          K1,K21,K22,K23,K24,K25,K26,K27,K28,P4
            WRITE(40,'(10G11.3)')
     1          K3,K34,K12,K10,K2,K33,K29,K31,K30,K13
            WRITE(40,'(10G11.3)')
     1          K14,K15,K16,K17,K18,K19,K20,E4,K11,K32
            WRITE(40,'(6G11.3)')
     1          D10,D20,C10,C20,A01
```

Parameters are:

IYEAR:	year
IDOY:	day of year
IHOUR:	hour
IMIN:	minute
ISEC:	second
ICOV	coverage in percent
Channels K1 to K32	see table 1.1
D10 to A01:	single detector count rates

Note: Data are rates, not intensities, and given per second.

Accumulation time is 10 minutes.

No RTG correction: The data are not corrected for false entries due to neutrons and gamma rays from the radioisotope thermoelectric generator (RTG).

Flag -707 marks data gaps

3.2 Caveats

1. Only rates C are given, since no simple estimate of the intensities can be done. Intensities (I) must be derived by dividing through the response factor G_i, and by correcting through pulse height analysis.

$$I = C/R_i \tag{3.1}$$

   Note that several response factors are only applicable to the daily averages PHA corrected data (check against our webpage):

http://www.ieap.uni-kiel.de/et/ag-heber/cospin/

2. Background fluxes of K1 (P1) are a combination of components, including a high RTG background rate. This channel should be used only during event times.

3. On 10 min averages some of the channels have limitations because of RTG background. Very slow increases are a sign that background levels are reached (a few percent per year).

   ==========
   GET LOW FLUX VALUES FROM THE PI ON LONGER ACCUMULATION PERIODS
   ==========

Send request to the KET PI
Send request to the KET technical manager

4. Fluxes of K11 (E12) and K13-K20 (E4) below 2.0e-4 and 2.5e-3, respectively, are a combination of different components including RTG background. The best known corrections are described in Heber et al. [1999, 2001], Rastoin [1995].

   ==========
   Levels below 3.0e-3, 2.5e-3 should not be considered.
   ==========

5. Fluxes of K32 (E300) are contaminated by high energy protons. Reliable fluxes need an PHA correction on longer accumulation periods (see also Clem et al., 2002).

6. Determination of the intensities of K29 (A116) needs a PHA correction on longer accumulation periods (several hours).

7. Time periods when KET is saturated or is working in a "calibration mode" have been omitted:

   eg. March event 1991

   peak fluxes in the June to August period 1991

   Jovian encounter.

8. Data for the Jovian encounter are available on a 4 min base.

   ==========
   Caution: Very high fluxes for KET !!!!
   ==========

Chapter 4

Daily averages readme

The daily averaged file KET.DAILY contains a subset of KET coincidence channels which have been corrected by using pulse height analysis (see section 2)

4.1 Record format for the KET

The KET file was written on a VMS machine using Fortran 77 routines. The format used is:

```
      IMPLICIT REAL(K)
      WRITE(40,'(5I5,F6.1,8G12.3/8G12.4/5G12.4)')
     +          iyear,idoy,ihour,iminute,isecond,coverage,
     +          K3,EK3,K34,EK34,K12,EK12,K10,EK10,          ! Protons
     +          K33,EK33,K29,EK29,K31,EK31,K30,EK30         ! Helium
     +          E4,EE4,K32B,EK32B    ! Electrons
     +          A01                                        ! Anticoincidence
```

Parameters are:

IYEAR:	year
IDOY:	day of year
IHOUR:	hour of day
IMINUTE	minute of hour
ISECOND	second of minute
COVERAGE	coverage in percent
KET channel	as in table 1.1.
A01	count rate of the anticoincidence

Note: Data are rates, not intensities, and given per second.

Accumulation time is 1 day.

Flag -707 marks data gaps or less than 4 entries in PHA selection.

K32(b) corresponds to a subchannel of K32, which minimizes background contribution due to energetic protons [Rastoin, 1995].

Bibliography

R. Brun, F. Bruyant, M. Maire, A. C. McPherson, and P. Zanarini. *GEANT3*. CERN DATA HANDLING DIVISON, 1987. (DD/EE/84-1).

J. Clem, P. Evenson, and B. Heber. Cosmic Electron Gradients in the Inner Heliosphere. *Geophysical Research Letters*, page in press, 2002.

B. Heber. *Modulation galaktischer kosmischer Protonen und alpha-Teilchen in der inneren dreidimensionalen Heliosphäre: Messungen des Kiel Electron Telescopes an Bord der Raumsonde Ulysses*. PhD thesis, Christian-Albrechts-Universität Kiel, 1997.

B. Heber, A. Raviart, P. Ferrando, H. Sierks, C. Paizis, H. Kunow, R. Müller-Mellin, V. Bothmer, and A. Posner. Determination of 7-30 MeV electron intensities: Ulysses COSPIN/KET results. In *Proc. 16th International Cosmic Ray Conference, Salt Lake City, Utah, USA, August 17-25, 1999*, volume 7, page 186, 1999.

B. Heber, P. Ferrando, A. Raviart, C. Paizis, R. Müller-Mellin, H. Kunow, M. S. Potgieter, S.E.S. Ferreira, and H. Fichtner. On the determination of the γ-ray contribution in the 3-10 MeV KET electron channel along the Ulysses trajectory. In *Proc. 27th ICRC*, page 2255, 2001.

C. Rastoin. *Les électrons de Jupiter et de la Galaxie dans l'heliosphere d'apres l'experience KET a bord de la sonde spatiale ULYSSE*. PhD thesis, Saclay, 1995.

H. Sierks. Auswertungen der Eichmessungen des Kieler Elektronen-Teleskops zur Erstellung von Energiespektren an Bord der Raumsonde ULYSSES (International Solar Polar Mission). Master's thesis, Christian-Albrechts-Universität Kiel, 1988.

J.A. Simpson, J.D. Anglin, A. Barlogh, M. Bercovitch, J.M. Bouman, E.E. Budzinski, J.R. Burrows, R. Carvell, J.J. Connell, R. Ducros, P. Ferrando, J. Firth, M. Garcia-Munoz, J. Henrion, R.J. Hynds, B. Iwers,

R.M. Jacquet, H. Kunow, G.A. Lentz, R.G. Marsden, R.B. McKibben, R. Müller-Mellin, D.E. Page, M.A. Perkins, A. Raviart, T.R. Sanderson, H. Sierks, L. Treguer, A.J. Tuzzolino, K.-P. Wenzel, and G. Wibberenz. The ULYSSES cosmic-ray and solar particle investigation. *Astron. Astrophys. Suppl.*, 92(2):365–399, 1992.

J. D. Sullivan. Geometrical Factor and directional Response of single and multi-element Particle Telescopes. *Nucl. Instr. and Meth.*, 95:5–11, 1971.

ReadMe for Ulysses KET Full Resolution Data Set Files

The KET full resolution data set contains readout-by-readout values of all science data quantities returned from the Ulysses COSPIN KET. The data set consists of one set of 3 files for each day in which data were returned during the Ulysses mission. If no data were returned during a day or the instrument has been operated in calibration mode, no files have been generated for that day. The 3 files each contain a distinct type of measurement returned by the KET. The pulse-height analysis (PHA) files include some base (unconverted) data in the form of PHA channels that are used to derive the physical unit quantities (energy losses, photon numbers, etc.).

Detailed descriptions of the content and format of each file type are given in header files. For energy ranges, particle types, and more details concerning the data quantities reported, see "A&A Article" on the UDS COSPIN Home Page (http://helio.estec.esa.nl/ulysses/archive/cospin.html) which reproduces Simpson et al., Astron. Astrophys. Suppl. Set: 92, 365-399 (1992).

The file naming convention is

ucosket[I][YEAR][DOY].[FILETYPE]

where YEAR = year (range 1990 – 2009)
DOY = day of year (Jan.1 = 001)
I = Version number of data
FILETYPE is one of the following

int: contains start-times, accumulation intervals, and counts for the spin-averaged coincidence counting rates, each of which are recorded in the spacecraft superformat.

Accumulation intervals are synchronized to the spacecraft spin rather than to the telemetry sequence. Thus each accumulation interval corresponds to an integral number of spins, but the number of spins (and thus seconds) in an accumulation interval varies from readout to readout, usually in a cyclic pattern determined by beating between the length of the telemetry cycle (determined by the telemetry bit rate) and the spacecraft spin period.

Energy ranges and particle types are given in the UDS KET Usernotes at http://.

pha: Definition and interpretation of quantities in this file is complex. See Simpson et al. (1992) for a description of the PHA capabilities of the KET.

This file contains results of **pulse-height analysis** (PHA) of signals produced by an incident particle in the semiconductors D1 and D2, the two Cherenkov C1 and C2 and the scintillation S2 as raw PHA channels. To insure accuracy of the conversion from

channel to energy loss or photon number, a calibration of the system on the detectors is measured by the pulse of relativistic protons performed monthly.

sect: contains start-times, accumulation intervals for all sectors and for each sector in ms, and counts for the **8-sectored coincidence counting rate E4 and P4**, which responds to electrons in the approximate energy range ~2-7 MeV and protons in the energy range from 5.4 to 25 MeV, respectively.

As for the spin-averaged rates, accumulation intervals are spin-synchronous so that each accumulation interval corresponds to an integral number of spins.